Research Square

Preprints are preliminary reports that have not undergone peer review.
They should not be considered conclusive, used to inform clinical practice,
or referenced by the media as validated information.

Assessment of critical behavior in lacunar oxides of type perovskite

M. Noumi

noumimarwa1992@gmail.com

University of Sfax

R. Dhahri

University of Sfax

E. Dhahri

University of Sfax

E. K. Hlil

Université de Grenoble Alpes, CNRS, Grenoble INP, Institut Néel

Research Article

Keywords: lacunar oxides, Magnetocaloric effect, Modified Arrott, Short-interactions, Critical exponent

Posted Date: September 24th, 2026

DOI: https://doi.org/10.21203/rs.3.rs-10682503/v1

License: This work is licensed under a Creative Commons Attribution 4.0 International License.
Read Full License

Additional Declarations: No competing interests reported.

Assessment of critical behavior in lacunar oxides of type perovskite

M. Noumi[1], R. Dhahri[1], E. Dhahri[1], E.K. Hlil[2]

1. Laboratory of Applied Physics, Faculty of Sciences of Sfax, University of Sfax, PB 1171, 3000 Sfax, Tunisia.

2. Université de Grenoble Alpes, CNRS, Grenoble INP, Institut Néel, 38000 Grenoble, France.

Corresponding author: noumimarwa1992@gmail.com

Abstract:

The effect of vacancy creation on the crystal structure and critical behavior of perovskite was analyzed for the compound $La_{0.8-x}\square_xNa_{0.2-x}\square_xMnO_3$ (x=0.00 and x=0.075). The Rietveld refinement indicates that our samples are pure and crystallized in the $R\bar{3}c$ space group for both compounds. A linear reduction in network parameters as well as a monotonic reduction of the angel O-Mn-O with the increase of vacant sites takes place. The critical behavior has been resolved through isothermal magnetization measurements around the critical temperature T_C by different ways. Among the methods used, we find the modified Arrott graphs (MAP), the Kouvel-Fisher method (KF) and the critical isothermal analysis (CIA) to analyze the magnetization isotherms near the phase transition. The critical exponents obtained (β, γ and δ) reveal that the creation of a hole in the Lanthanum (La) and Sodium (Na) site changes the type of interaction. Our two compounds follow different models, confirming the existence of two types of interactions for x = 0.00 and x = 0.075.

The reliability of the critical exponent (β, γ and δ) has been verified by the universal scaling behavior of the isothermal magnetization near the phase transition temperature. The critical exponents found not only with those methods (MAP), (KF) and (CIA), but they also obey the theory of scaling. Our results confirm the good correlation between the critical behavior and the magnetocaloric effect (MCE).

Keywords: lacunar oxides; Magnetocaloric effect; Modified Arrott, Short-interactions; Critical exponent.

Introduction:

The richness of manganites facilitates the use in multiple fields; this advantage comes from the orbital interaction, the load and the network. This is reflected in the diversity of their properties, such as transport, magnetic, magnetoresistance (MR) and magnetocaloric effect (MCE) **[1–4]**. These materials undergo a combination of different phases, insulating, metallic and various magnetic phases; ferromagnetic, ferrimagnetic and rotating glass **[5]**. Specifically, lanthanum perovskites manganites have become potential candidates for refrigeration at different temperature ranges **[6–9]**.

Thus, the most usable manganites are $LaMnO_3$ after doping or the creation of holes of several variations due to its ionic radius, its orbital order **[10]**, its order of charge **[11.12]**, and its phase separation **[13]** which can be attributed to a complex interaction between, the super-exchange antiferromagnetic interaction, the double exchange ferromagnetic interaction and the Jahn-Teller distortion.

In addition, these compounds have attracted a lot of attention due to the strong coupling between the structure and the magnetism of phenomena including the paramagnetic-ferromagnetic transition. Extensive research has indicated that the double exchange interaction (DE) between Mn^{3+} and Mn^{4+} can exhibit a PM-FM transition around the Curie temperature **[14 –18]**.

A very detailed study of the critical phenomena from the magnetic properties and entropy of the samples $La_{0.8-x}\square_xNa_{0.2-x}\square_xMnO_3$ (x = 0.00 and x= 0.075) is reported. Critical exponents are estimated by isothermal magnetization measurements around the Curie temperature using various techniques such as the modified Arrott plot (MAP), the Kouvel-Fisher method (KF) and the critical isothermal analysis (CIA).

Magnetic interactions can be described by four models: mean field, Heisenberg 3D, Ising 3D and tricritical mean field. The critical values of the exponents (β, γ and δ) associated with the transition then place the material in a certain class of universality which depends on the range of interactions of magnetism.

The 3D-Heisenberg and 3D-Ising models are a statistical model used to study critical points and magnetic phase transitions. In these models, short-range exchange interactions exist between the spins with the presence of significant spin fluctuations in the vicinity of T_C. As much as the mean field model describes long-range exchange interactions with negligible critical fluctuations near the Curie temperature T_C.

Then an intrinsic relation between the critical phenomena and the magnetocaloric properties, that is to say the magnetic entropy as well as the relative cooling power are analyzed and determine the critical exponents.

2. Experimental method:

In our work, we choose the sol gel route for sample preparation because of the advantages of this method. The synthesis is done at low temperature, obtaining very pure materials with great homogeneity using the following precursors: La $(NO_3)_3 \bullet 6H_2O$, Mn $(NO_3)_2 \bullet 4H_2O$ and $NaNO_3$ of nominal purity not less than 99.99%) **[19]**.

3. Results and discussion:

Structural analysis:

The crystallographic structure was determined by refinement of X-ray diffractograms using the Rietveld method **[20]** by the Full Prof program. The refined diffractograms shown in **Figure 1** show that the samples $La_{0.8-x}\square_xNa_{0.2-x}\square_xMnO_3$ with $x = 0.00$ and $x = 0.075$ are crystallized in the rhombohedral structure with the space group $R\bar{3}c$.

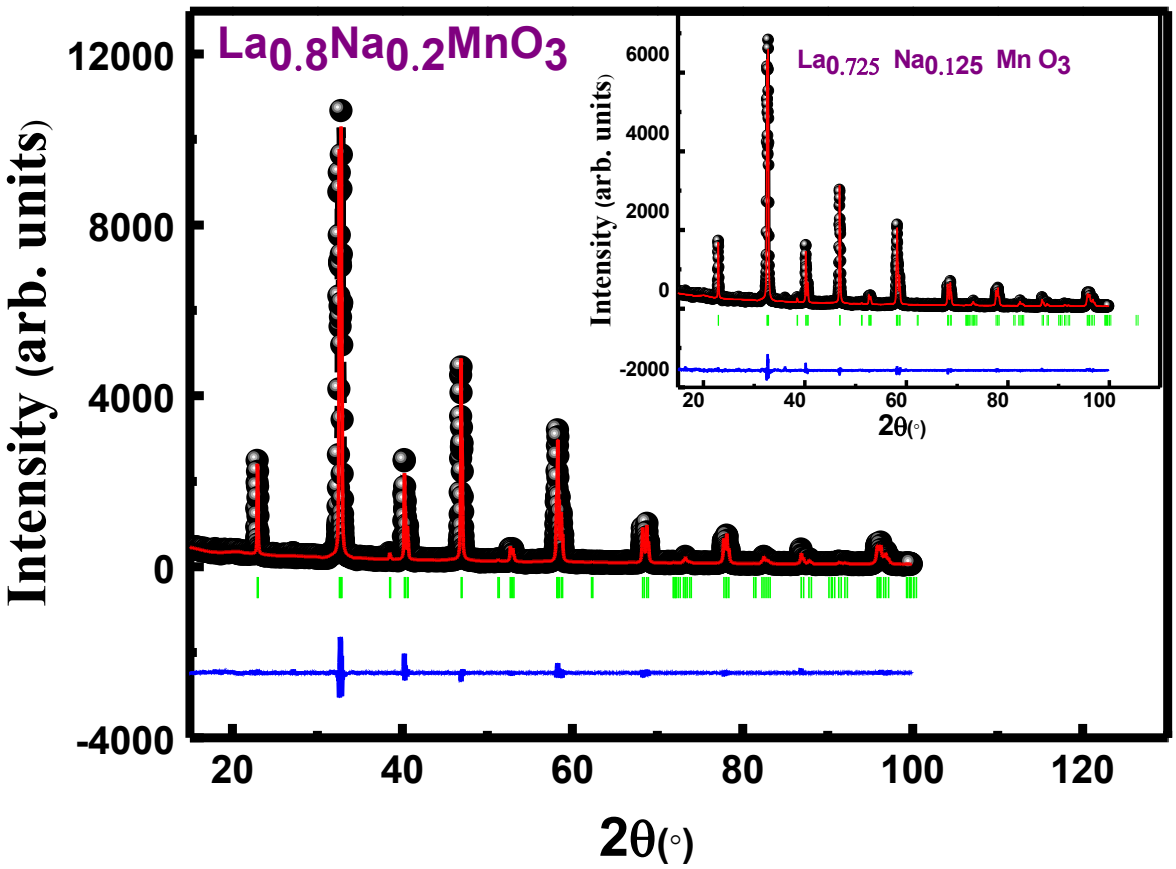


Fig.1: X-ray diffractograms for the compounds $La_{0.8-x}\square_x Na_{0,2-x}\square_xMnO_3$ (x=0.00, x=0.075).

The various refined network parameters, unit cell volume, and reliability factors (R) for the two samples are listed in **Table 1**. Typically, we report the R_f factor and the Bragg factor R_B; these factors refer to the crystallographic tuning and the tuning of consecutively reflected intensities.

Table 1 also shows the network parameters (a, b and c), and the unit cell volume (V) with the creation of gap rates. From this table, we notice that the creation of vacancies leads to the increase in the volume of the elementary cell, this increase explained by the increase in the number of Mn^{3+} ions and the decrease in that of Mn^{4+} ions, which generates a decrease in the mean radius of site B.

Table 1: Crystallographic parameters of compounds $La_{0.8-x}\ \square_x\ Na_{0,2-x}\ \square_x MnO_3$ (x=0.00, x=0.075).

	a (Å)	b (Å)	c (Å)	v (Å^3)	R_B	R_F	Mn-O	O-Mn-O
***x* =0.00**	5.492	5.492	13.327	348.219	2.36	2.01	1.953	89.06
***x*=0.075**	5.501	5.501	13.341	349.607	2.17	2.42	1.958	90.90

A slight variation of the parameters of the network leads to modifications of the bond lengths (Mn-O), and therefore the angles of the bonds (O-Mn-O) as indicated in **Table 1**. The VESTA software was used to characterize the distances (Mn-O) between Mn ions and closest neighbors of oxygen ions as well as bond angles (O-Mn-O). The coordination octahedral of Mn is shown in **Figure 2** for the compound $La_{0.8}Na_{0.2}MnO_3$.

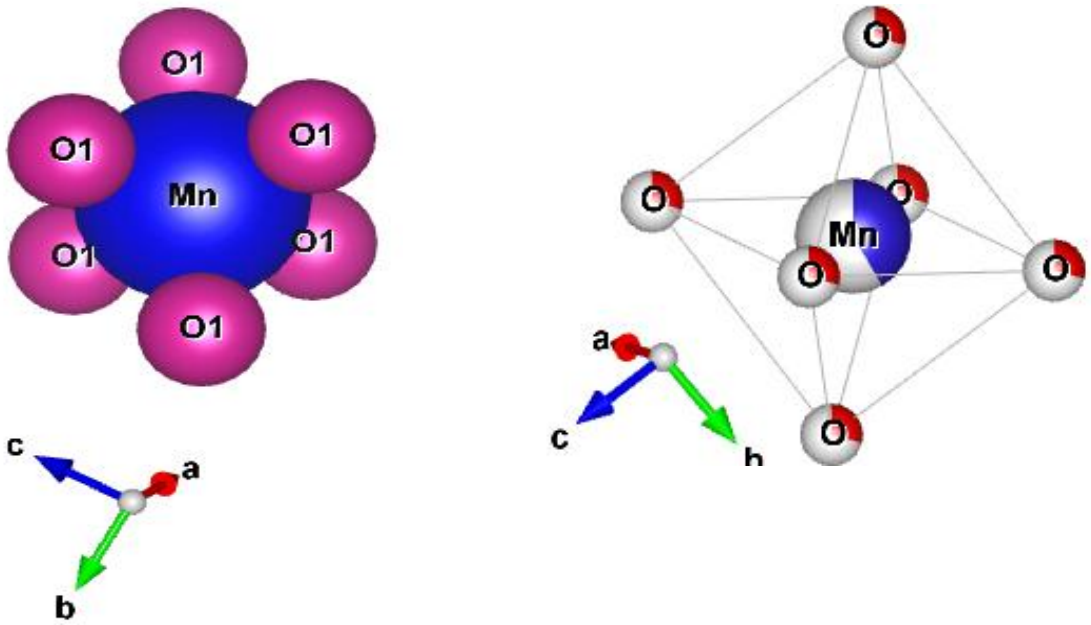


Fig.2: The coordinate of polyhedral of Mn in $La_{0.8}Na_{0.2}MnO_3$ compound.

Critical behavior study:

After refining the samples and ensuring that they are pure, we measure the magnetization as a function of the magnetic field applied at different temperatures to obtain the isotherms M (H, T) from which we determine the critical exponents.

The critical behavior in compounds associated with magnetic phase transition has been investigated by magnetization isotherms.

Critical exponents are deduced using various techniques such as the Kouvel - Fisher graphical Arrott and critical isotherm technique. One approach to understanding the nature of the FM – PM transition is to study its critical behavior. In manganites, magnetic interactions can be generally described by four models: mean field **[21]**, 3D Heisenberg **[22]**, 3D Ising and Tricritical mean field **[21]**. The values of the critical exponents (β, γ and δ) associated with the transition then put the material in a certain class of universality which depends on the range of magnetism interactions are illustrated in **Table 2** as well as a bibliographic collection of critical exponents which is determined experimentally **[23-25]**.

Table 2: Critical exponents β, γ and δ using various technique

	T_C (K)	β	γ	δ	references
Mean field theory	-	0.5	1	3.0	[21]
Tricritical mean field theory	-	0.25	1	5	[22]
Heisenberg 3D theory	-	0.365±0.003	1.336±0.004	4.80±0.04	[21]
Ising 3D theory	-	0.325±0.002	1.241±0.002	4.82±0.02	[21]
$La_{0.8}Ca_{0.2}Mn O_3$	181	0.325	1.180	4.826	[23]
$La_{0.7}Ba_{0.3}Mn O_3$	311	0.54	1.04	3.08	[24]
$La_{0.6}Ca_{0.4}Mn O_3$	268	0.287	0.989	4.896	[25]

The reported values for the critical parameters of various perovskites manganites are controversial, spanning the range between those corresponding to the short-range Heisenberg model (β = 0.36, γ = 1.336 and δ = 4.8), 3D Ising model (β = 0.325, γ = 1.241 and δ = 4.82) and those corresponding to the long distance mean field theory (β = 0.5, γ = 1, and δ = 5) **[26-29]**.

The parameters of the critical exponents are defined mathematically according to the following equations:

- β is the exponent associated with spontaneous magnetization below T_C (absence of the magnetic), which is defined by the following relation (1):

$$M_S(T) = M_0(-\varepsilon)^{\beta}, \quad \varepsilon < 0 \qquad (1)$$

$\varepsilon = (T - Tc)/T_C$ is the reduced temperature and M_0 is a critical amplitude.

- γ is the exponent associated with the isothermal magnetic susceptibility above T_C given by equation (2):

$$\chi_0^{-1}(T) = \left(\frac{h_0}{M_0}\right)\varepsilon^{\delta}, \varepsilon > 0 \qquad (2)$$

χ_0^{-1} is the inverse of the susceptibility in zero field, h_0 a critical amplitude.

- δ is the exponent linked to the critical isotherm (T = Tc) defined by equation (3):

$$M = DH^{1/\delta}, \quad \varepsilon = 0 \qquad (3)$$

Where H is the internal field and D is critical amplitude.

Scaling analysis:

A phase transition occurs at T_C where the material goes from a PM condition to a condition greater than T_C to a FM state less than T_C. Studies are conducted in the phase transition region. These materials can be characterized according to their transition temperature and their critical exponents, which are linked to parameters such as spontaneous magnetization and the initial susceptibility close to the transition temperature.

In addition, the dependence of the field and the temperature of the magnetization in the regime critique obey a scale relation, which can be expressed according to the hypothesis scale by:

$$\boldsymbol{M(H,\varepsilon) = \varepsilon^{\beta} f_{\pm}\left(\frac{H}{\varepsilon^{\beta+\gamma}}\right)} \qquad (4)$$

Where f_+ for T> T_C and f_- for T <T_C are regular analytical functions.

The exact values of the critical exponents and the temperature of Curie T_C were determined from the Arrott - Noakes traces.

"Scaling" and "universality" are the concepts developed to understand critical phenomena. Scaling means that systems in the vicinity of critical points with self-similarity properties are invariant by transformation of scale.

To determine the critical exponents of our samples, several conventional techniques can be used from the magnetization according to the magnetic field applied under different temperatures according to one of the following procedures:

- Arrott tracks **[30]**
- Arrott-Noakes plots (modified Arrott plots) **[31]**
- Kouvel-Fisher plots **[32]**
- Critical isotherm

The measurements of the magnetization as a function of the magnetic field applied at different temperatures on either side of the Curie temperature are indicated on the Arrott curves **[30]** (M^2 vs H / M) presented in **Figure 3 and Figure 4** for the compounds $La_{0.8-x}\square_xNa_{0.2-x}\square_xMnO_3$ ($x = 0.00$ and $x = 0.075$).

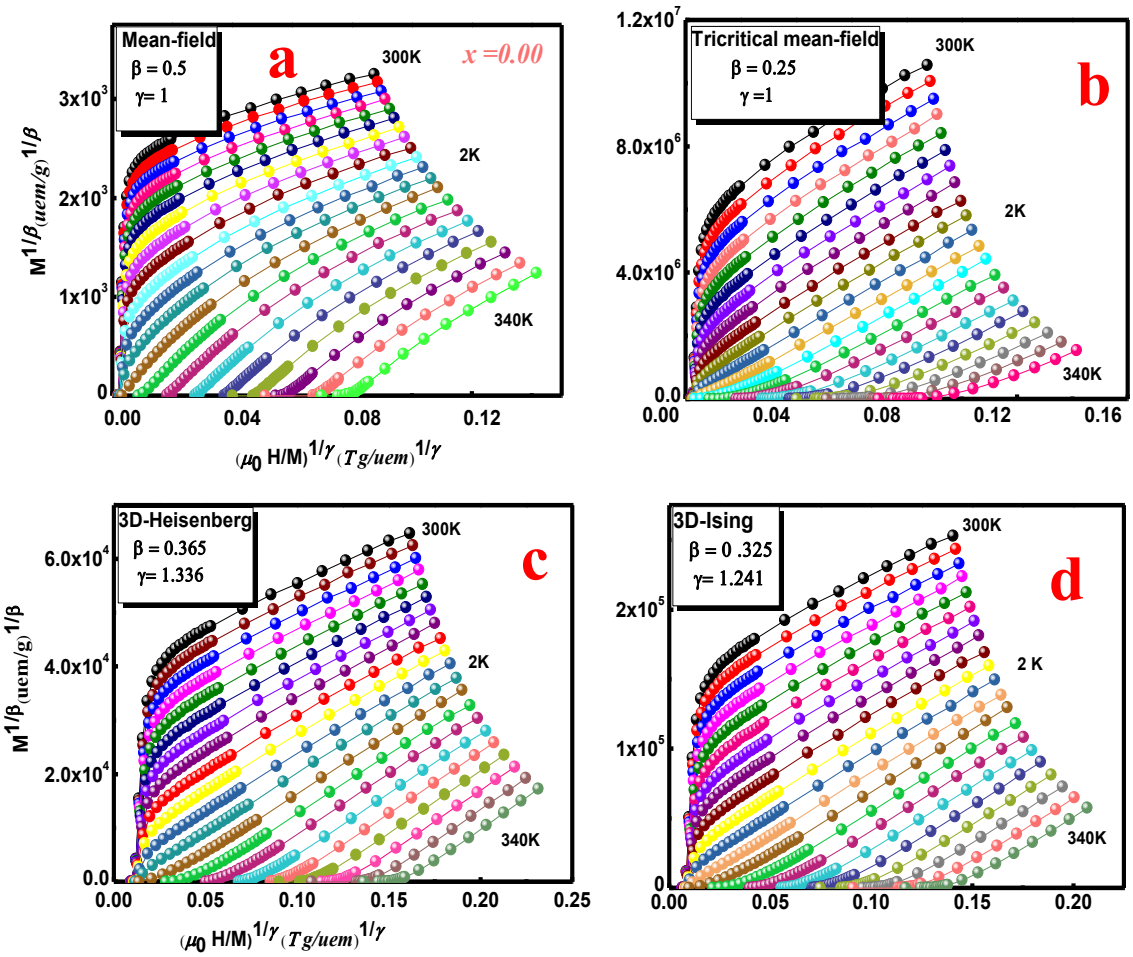


Fig.3: Modified Arrott-plots for $La_{0.8}Na_{0.2}MnO_3$ compound using different models; **(a)** mean field model, **(b)** Tricritical mean field model, **(c)** 3D-Heisenberg m **(d)** 3D-Ising model model.

A ferromagnetic behavior under the Curie temperature is determined from the M (T) measurements. The phase transition would be clearer if we drew different models around T_C. All of the curves in these charts behave in a non-linear fashion with a downward curvature. According to this criterion, the magnetic transition has a negative slope so the H / M curves as a function of M^2 are of the first order, otherwise the slope is positive, so H / M as a function of M^2 is of second order. We can see from the curves that our compounds have a positive slope indicating that the transition is second order.

According to the criterion proposed by Banerjee **[33]**, the Arrott plot assumes that the critical exponents follow the average field theory (β = 0.5, γ = 1, δ = 3). This plot was used to be a conventional method for determining critical exponents, since the M^2 vs H / M isotherms are a set of parallel lines around T_C.

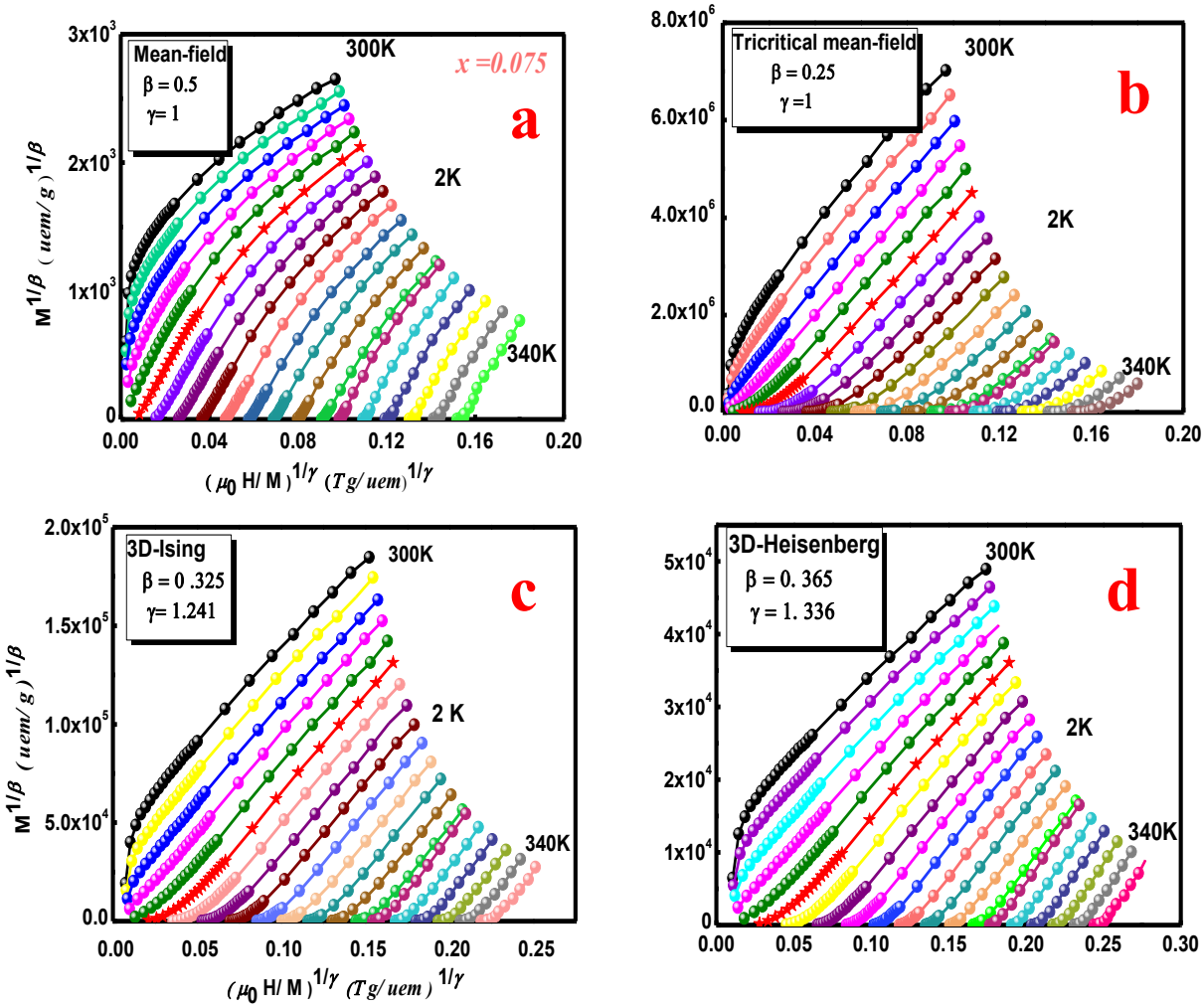


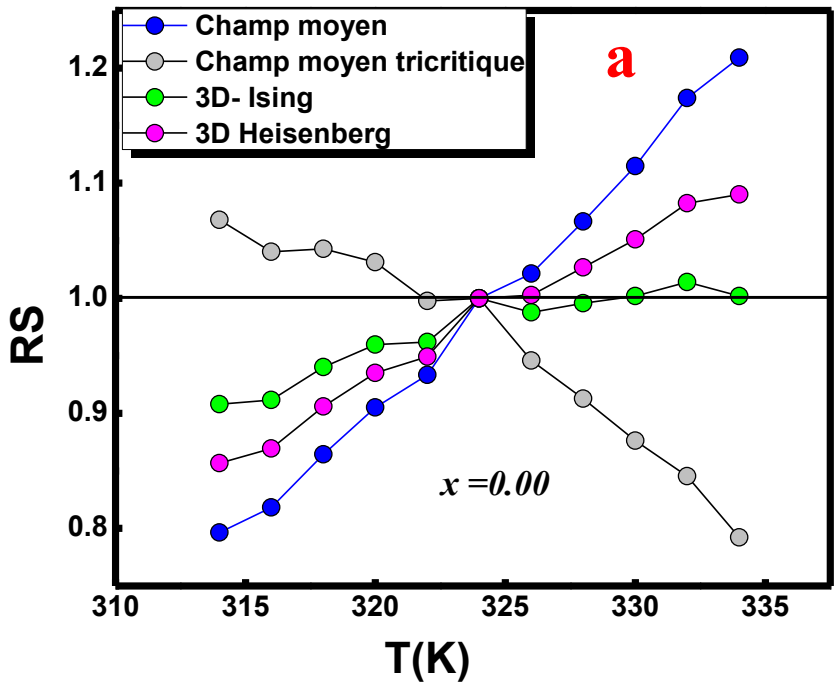
Fig.4: Modified Arrott-plots for $La_{0.725}Na_{0.125}MnO_3$ compound using different models; **(a)** mean field model, **(b)** Tricritical mean field model,**(c)** 3D-Ising model, **(d)** 3D-Heisenberg model.

The Arrott plots assume that the critical exponents follow the mean field theory ($\beta = 0.5$, $\gamma = 1$, $\delta = 3$). This traditional method has been used to identify exhibitors. Thus, three types of exponents are cited, the 3D Heisenberg model ($\beta = 0.365$, $\gamma = 1.336$ and $\delta = 4.80$), the 3D Ising model ($\beta = 0.325$, $\gamma = 1.241$ and $\delta = 4.82$), and the tricritical mean field model ($\beta = 0.25$, $\gamma = 1$ and $\delta = 5$), which are exposed respectively in **Figure 3** and **Figure 4** for compounds x=0.00 and x=0.075.

From the curves, we choose the model which has linear and parallel straight lines for a respectable range of the magnetic field even for strong fields.

This is confirmed by the variation of the relative slope RS (slope / slope at T_C) as a function of the temperature. A primary forecast of the initial values of the critical exponents (β, γ) so we determine these values by precision from the Arrott-Noakes plot M_S (T, 0) and χ_0^{-1}.

As shown in the **Figure 5**, the RS of the compounds $La_{0.8}Na_{0.2}MnO_3$ and $La_{0.725}Na_{0.125}MnO_3$ using several methods: tricritical mean field, the 3-D Heisenberg model, the mean field model and the 3-D Ising.



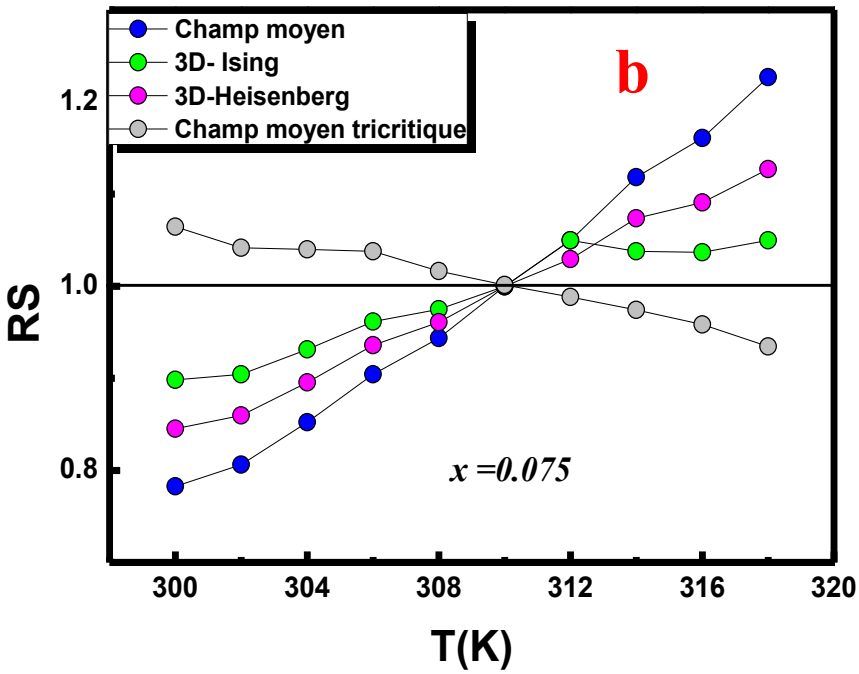


Fig.5. Relative slope (RS) of **(a)** x = 0.00, and **(b)** x = 0.075 sample as a function of temperature defined as RS = S(T)/S(T_C).

The most appropriate model should be the one with a RS value very close to the unit.

Therefore, we can deduce that the 3D Ising model is the best model that can describe the transition for the *x*=0.00 sample, while the tricrtical mean filed model for the *x*=0.075 sample.

On the basis of the models obtained from RS, we were able to calculate the values of the spontaneous magnetization Ms (T) and the inverse of susceptibility χ_0^{-1}.

The precise values of the critical exponents and the Curie temperature T_C are deduced from the Arrott-Noakes plots **[34]** (also called modified Arrott plots).

In this technique, the data M = f (H) are converted to sets of isotherms $M^{1/\beta} = f((H/M)^{1/\gamma})$ which depend on the following relation:

$$(H/M)^{1/\gamma} = (T - T_C) / T_1 + (M/M_1)^{1/\beta} \qquad (5)$$

Linear extrapolation on the right side of the upper field of the isotherm provides the values of Ms (T <Tc) and χ_0^{-1} $(T > Tc)$ on the y-axis at the origin on the axes $M^{1/\beta}$ and $(H/M)^{1/\gamma}$ respectively. Then, we fit these curves with the equations (1) and (2) to obtain the new values of β et γ corresponding to that of the optimal fit obtained (**Figure 6**).

The values of β = 0.42 ± 0.04 at T_C = 322.92 ± 0.51 K and γ = 1.08 ± 0.09 at T_C = 322.02 ± 0.76K for the compound $La_{0.8}Na_{0.2}MnO_3$, β = 0.299 ± 0.01 at T_C = 306.18 ± 0.51 K and γ = 1.05 ± 0.06 at T_C = 307.22 ± 0.38K for the compound $La_{0.725}$ $Na_{0.125}MnO_3$.

These values are close to the critical exponent of the 3 D-Ising model and tricritical mean field model respectively.

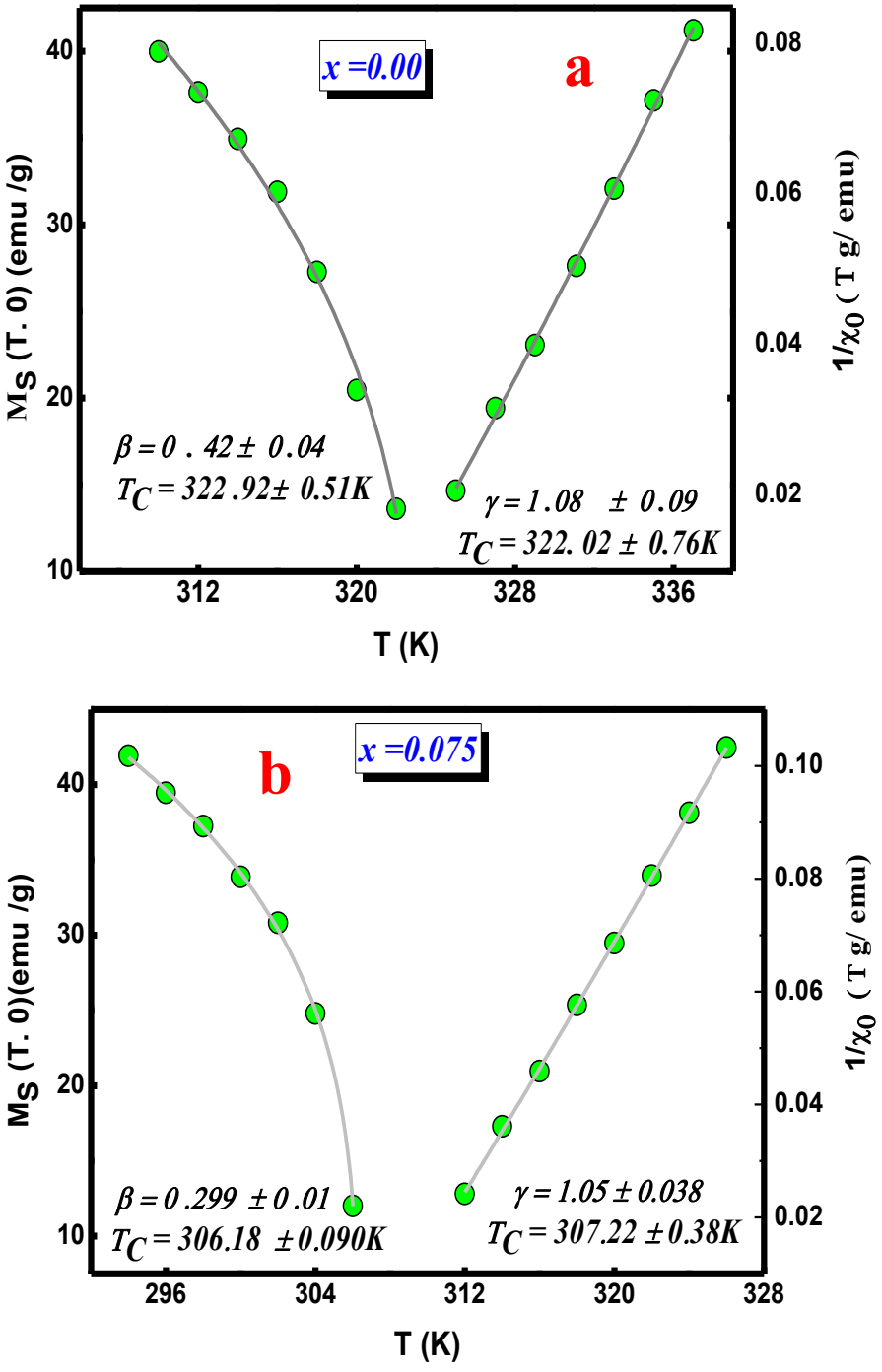


Fig.6: Temperature dependence of $M_s(T)$ and χ_0^{-1} determined from the modified Arrott plot for **(a)** x = 0.00, and **(b)** x = 0.075.

This confirms the existence of short-range antiferromagnetic and/or ferromagnetic interactions for x=0.00 and the existence of long-range interactions for x=0.075.
These results are detailed in **Table 3**.

Table3: Critical exponents of $La_{0.8}Na_{0.2}MnO_3$ and $La_{0.725}Na_{0.125}MnO_3$ using various techniques.

	Modified Arrott plot (MAP)			**Kouvel-Fisher (KF)**			**critical isotherm analysis (CIA)**	
x	**β**	**γ**	**T_C (K)**	**β**	**γ**	**T_C (K)**	**δ_{exp}**	**δ_{cal}**
00.00	0.42 ± 0.04	1.08±0.09	322±0.76	0.322±0.02	1.03±0.09	324±0.9	3.397	3.48
0.075	0.31±0.01	1.05±0.03	307±0.38	0.284±0.01	1.03±0.02	307±0.45	3.351	3.95

The Kouvel-Fisher plots:

To determine the critical exponents as well as T_C more precisely, we analyzed the data Ms (T) and χ_0^{-1} (T) using the Kouvel - Fisher Method (KF) according to the following equations:

$$\frac{M_S(T)}{dM/dT} = \frac{T-T_C}{\beta} \qquad (6)$$

$$\frac{\chi_0^{-1}(T)}{d\chi_0^{-1}/dT} = \frac{T-T_C}{\gamma} \qquad (7)$$

According to this method and using the curves of Ms (T) and χ_0^{-1} we have plotted Ms (T) $(dMs\ (T)\ /\ dT)^{-1}$ and $\chi_0^{-1}(d\chi_0^{-1}(T)/dT)$ as a function of temperature. These curves should directly give two straight lines with slopes 1/β and 1/γ respectively. The **KF** graphs for the three samples are shown in **Figure 7**.
When these straight lines are extrapolated to the ordinates equal to zero, the intersections on the T axis correspond to the Curie temperature. The results of fitting with the Kouvel-Fisher method give the exponents (β, γ) and T_C.

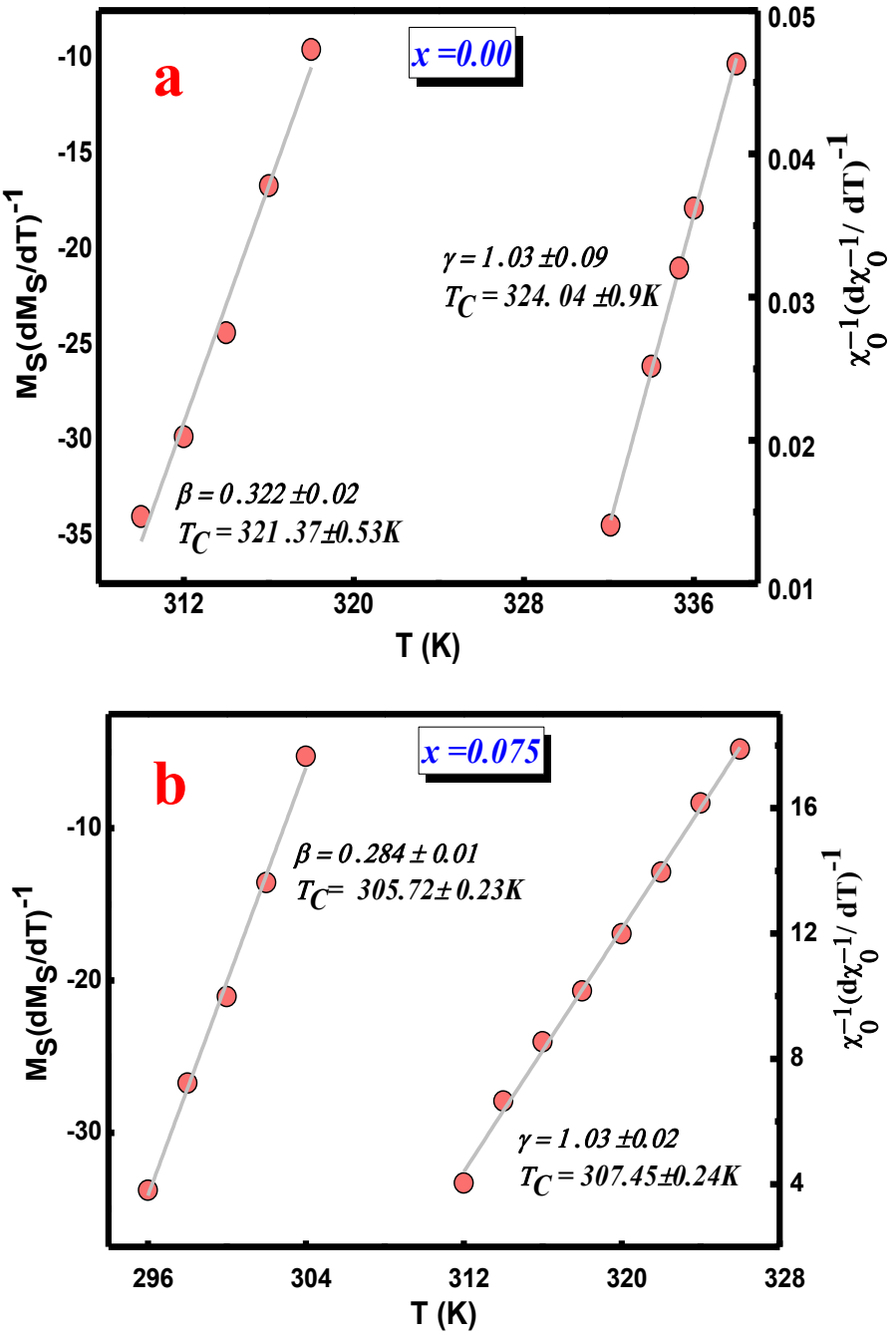


Fig.7: Kouvel-Fisher plots for M_s (T) and χ_0^{-1} plot of **(a)** x = 0.00, and **(b)** x = 0.075.

The values of the exponents obtained are very close to the values of the initial exponents, and the values determined from Ms(T) and χ_0^{-1}(T) fit very well. It is noted that the critical exponent and T_C values obtained by this method are in good agreement with those estimated by the modified Arrott plots (MAP) method.

Critical isotherm:

After solving the exponents β and γ, we specify the value of the critical exponent δ estimated from the variation of Ln(M) as a function of Ln(H) at the Curie temperature T_C which are presented in the **Figure 8**.

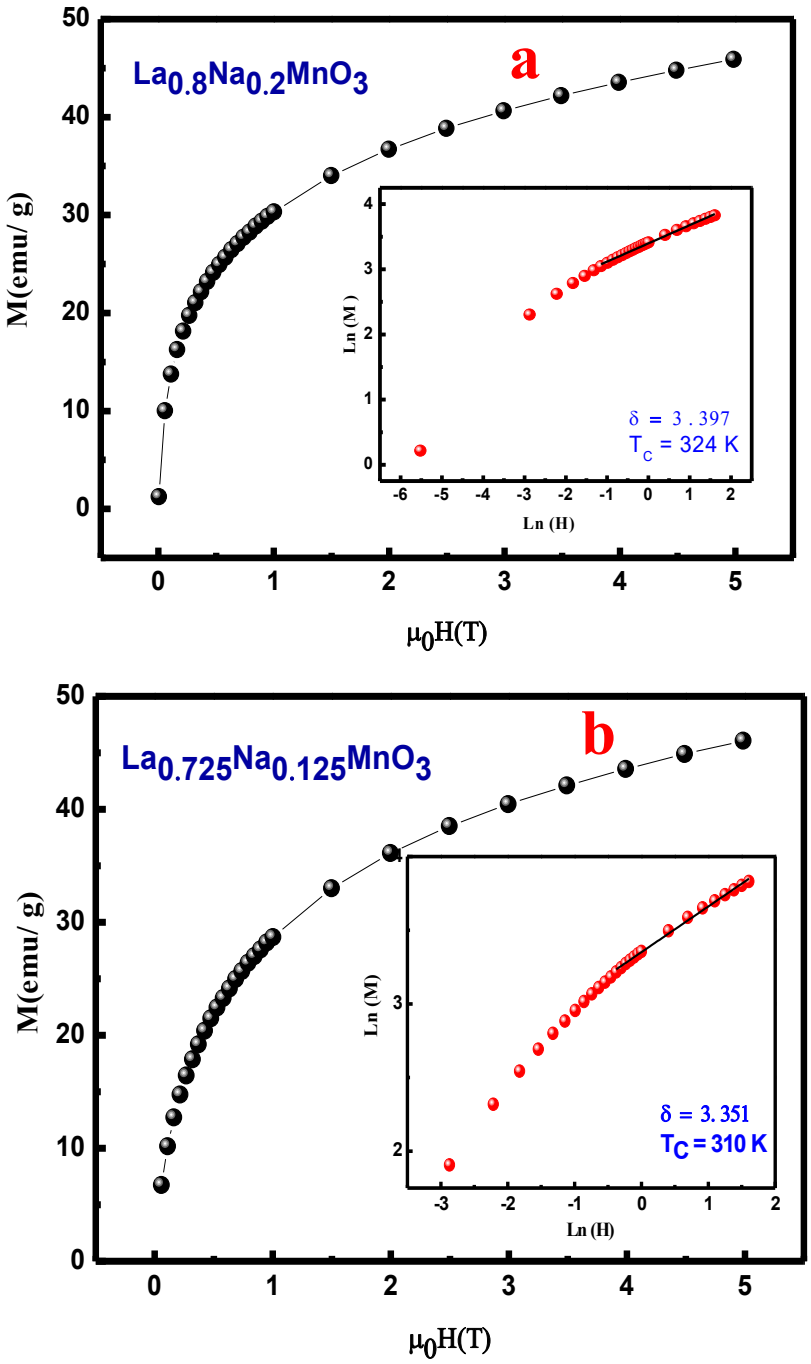


Fig.8: Critical isotherm at T=Tc in the $La_{0.8-x}\square_xNa_{0.2-x}\square_xMnO_3$ **(a)** x=0.00 and **(b)** x=0.075 compound in log-log scale.

The high field region of these curves is a line with slope 1 / δ. The value of δ was determined using β and γ according to equation 5:

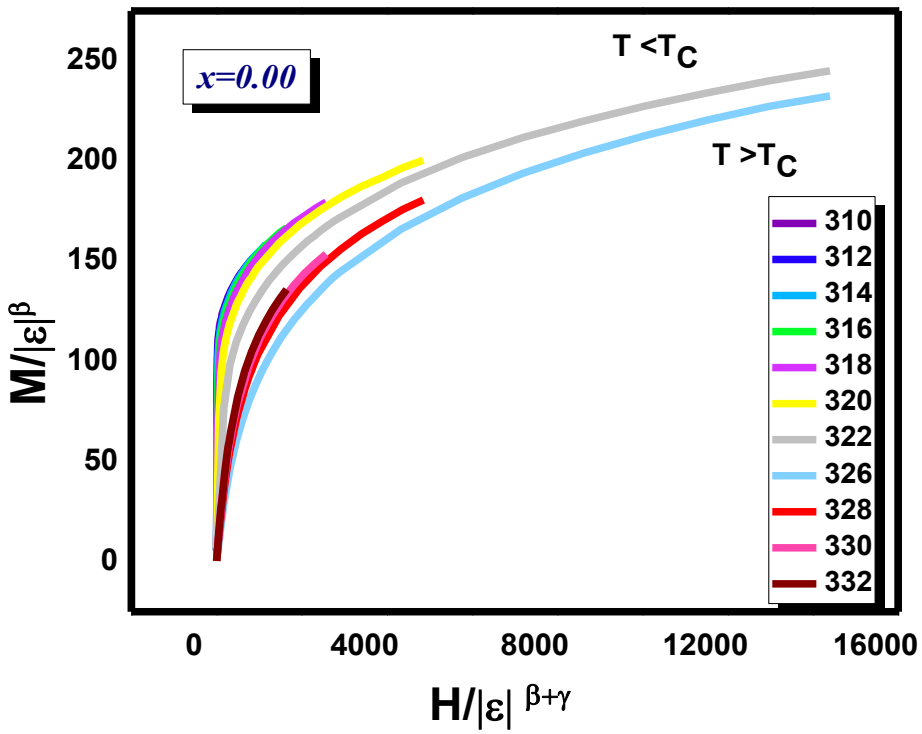
$$\delta = 1 + \frac{\gamma}{\beta} \qquad (8)$$

From this equalization, the δ values are calculated with the β and γ values obtained from the modified Arrott plot and the KF method (**Table 3**).

We notice that these values of δ are very close to those given by the Ising model for the compound$La_{0.8}Na_{0.2}MnO_3$ and tricritical mean filed for the deficient compound $La_{0.725}Na_{0.125}MnO_3$.

Ladder behavior:

To verify the validity of the critical exponents discovered experimentally, we have exploited the scaling law which assumes that the magnetization must obey the universal scaling behavior. The isotherms of the variation of $M /| \varepsilon |^{\beta}$ as a function of $H /| \varepsilon |^{\beta+\gamma}$ for temperatures lower than T_C ($T < T_C$) and the other of $T > T_C$ as designated in **Figure 9**.



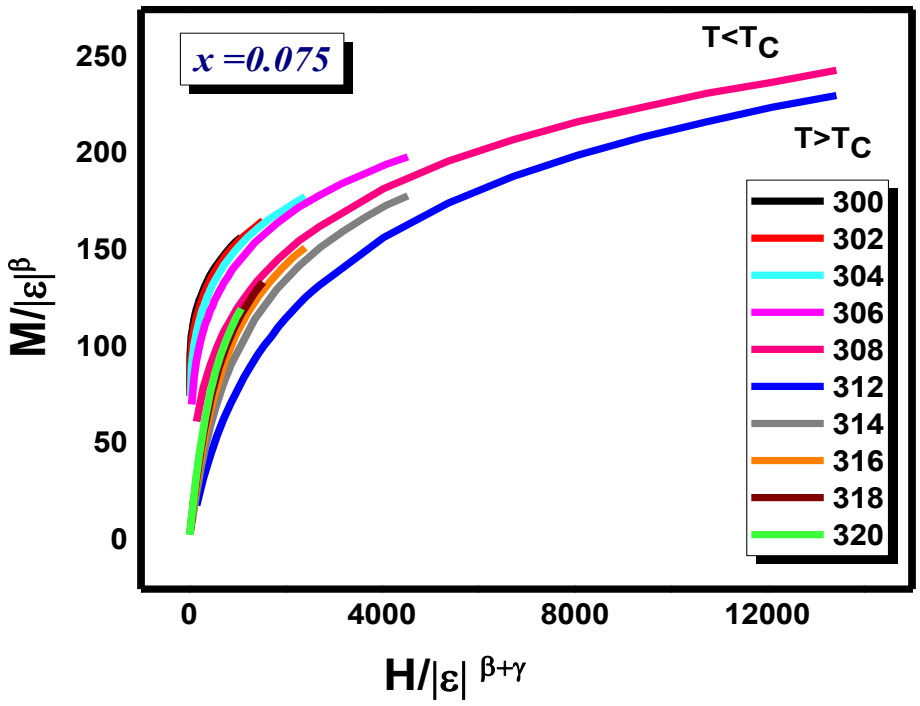


Fig.9: Scaling plots indicating two universal curves below and above T_C.

The graphs show the same data on a double logarithmic scale. In addition, the figure clearly shows that the scaling behavior is verified for the two samples, i.e. all the points are formed on two curves, one for $T < T_C$ and for $T > T_C$. Thus, the obtained values of the critical exponents and T_C are in agreement with the assumption of scale.

Correlation between critical exponents and magnetocaloric effect:

The importance of $-\Delta S_M$ induced by the magnetic field, introduced that the materials can be used for practical applications and refrigeration capacity (RCP) which makes them promising candidates for magnetic refrigeration **[19]**. A universal law of the field **[35]** explains the correlation of magnetic entropy of materials and the second order phase transition parameter given by:

$$\Delta S_M \propto (\mu_0 H)^n \qquad (9)$$

In this formula n is a magnetic parameter **[35-36]** depending on the magnetic state of the studied compounds. On the **figure 10**, we have plotted the variation of $Ln(-\Delta S_M)$ as a function of $Ln(\mu_0 H)$ to find phenomenological model for our compounds.

This evolution turns out to be linear and the obtained values of n are 0.69 and 0.61 for $x = 0.00$ and 0.075 respectively.

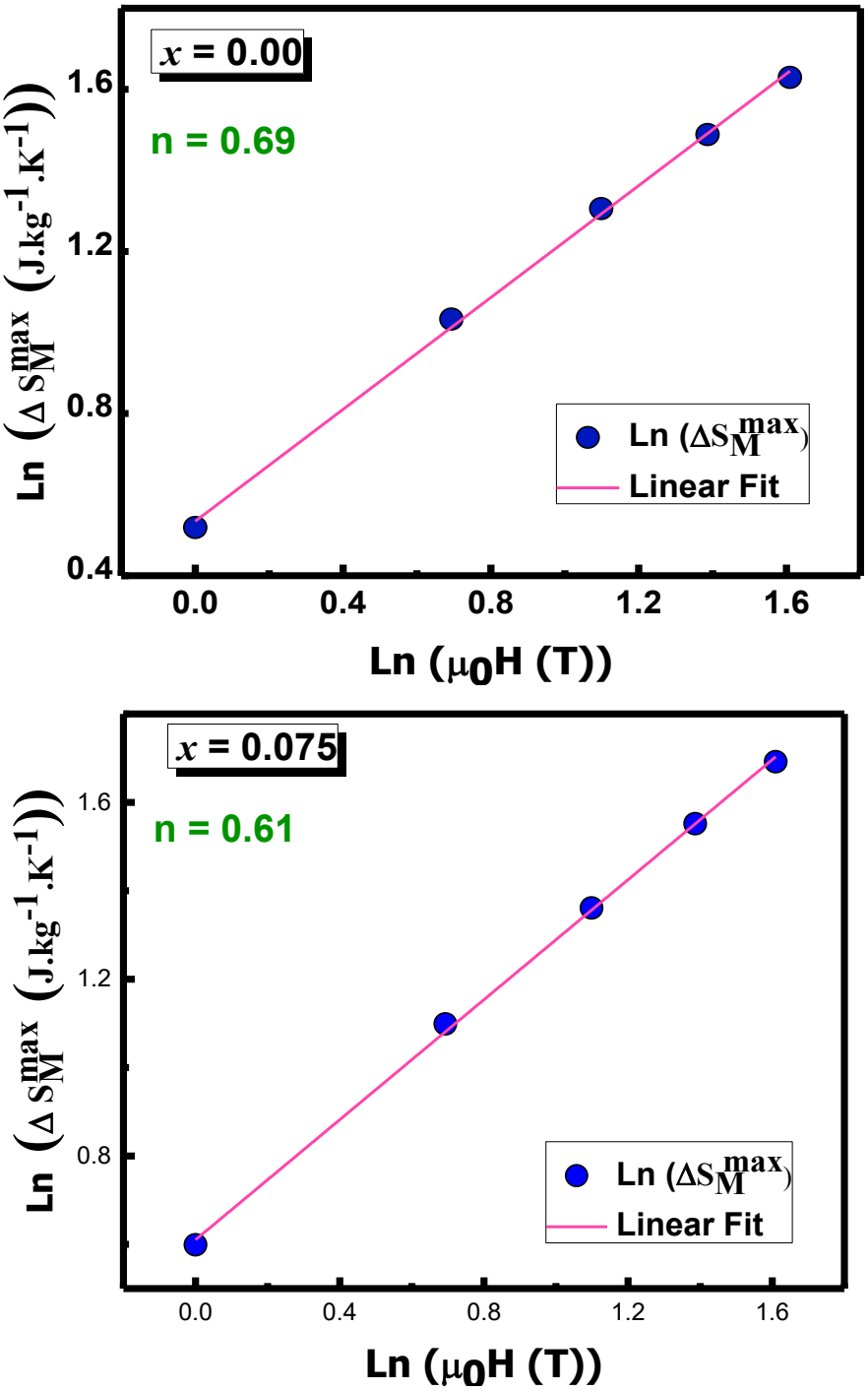


Fig.10: Field dependence of maximum magnetic entropy change for $La_{0.8-x}\square_xNa_{0.2-x}\square_xMnO_3$ with x = 0.00 and 0.075.

We notice that this exponent depends on the field in the temperature range to analyze. This suggests the existence of magnetic inhomogeneities **[37]**. Indeed, the values of n shows a variation can be explained by the law of Curie Weiss reflecting the greater sensitivity of the magnetic entropy to the change of external field in this temperature range.

Thus, we explain the correlation to the RCP field by power law written in the form **[38]**:

$$RCP \propto (\mu_0 H)^{1+1/\delta} \qquad (10)$$

δ is the critical exponent of the magnetic transition.

The **figure 11** shows the dependence on the RCP field so the values of δ are deduced from the adjustment (RCP vs.μ_0H) of plot corresponds to 3.58 and 3.54 for $La_{0.8}Na_{0.2}MnO_3$ and $La_{0.25}Na_{0.125}MnO_3$ respectively.

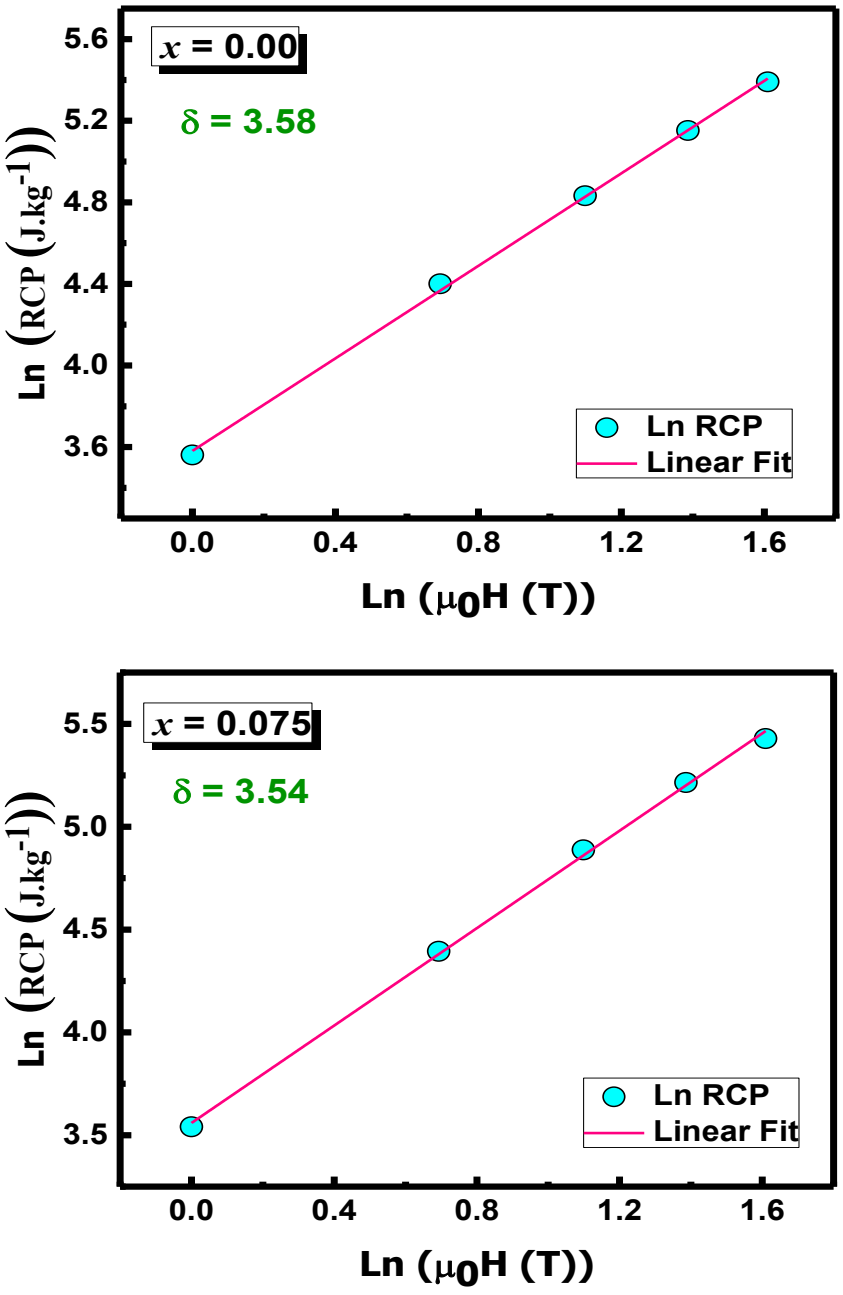


Figure 11: Variation of RCP vs. μ_0H of $La_{0.8-x}\square_x Na_{0.2-x}\square_x MnO_3$ (x = 0.00 and 0.075) compounds.

Especially when T = Tc, a relation between the exponent n and the critical exponents β and γ are established as follows **[39]**:

$$\mathbf{n\ (T_C) = 1 + \frac{\beta - 1}{\beta + 1}} \qquad (11)$$

Since $\beta\delta = \beta + \gamma$ **[40]**, Eq. (11) can be rewritten as:

$$\mathbf{n\ (T_C) = \ 1 + \frac{1}{\delta}\left(1 - \frac{1}{\beta}\right)} \qquad (12)$$

Following the equations (11) and (12), we extracted the value of **n** and **δ** in order to determine the critical exponents (β and γ) which are (0.47 and 1.20) for $La_{0.8}Na_{0.2}MnO_3$ and (0.42 and 1.06) for $La_{0.725}Na_{0.125}MnO_3$. It is marked that the values of the critical exponents obtained in the magnetic entropy field evolve and linked with those corresponding to the models suitable for the two samples.

Conclusion:

In summary, the structural study showed that both compounds crystallize in the rhombohedral structure with the $R\bar{3}c$ space group. We analyzed the effect of the creation of the deficit site on the critical behavior and the correlation with the magnetocaloric effect.

The critical parameters are studied using classical methods of phase transition analysis, such as the Kouvel Fisher method, the modified Arrott diagram and the critical isothermal analysis; we determined the critical exponents β, γ and δ. The validity of our critical exponents is confirmed by scale analysis.

The values of the estimated critical exponents are consistent with the 3D-Ising model for x= 0.00 and the Tricritical mean field model for x = 0.075. This change in the universality class is due to the relevant disorder introduced by the creation of the gap rate in Site A.

Another method to obtain the exponents β, γ and δ; they have been extracted from the MCE analysis and were found to obey the scaling theory. These results prove the intrinsic relationship between MCE properties and the universality class.

Refrences:

[1] Y. Tokura, and N. Nagaosa Science, Orbital Physics in Transition-Metal Oxides, 21 Apr, Vol. 288.5465. pp. 462–468 (2000).

[2] J.B. Goodenough, Prog. Solid State Chem. 5.145.(1972).

[3] H. Wang, X. Zhang, M.F. Hundley, J.D. Thompson, B.J. Gibbons, Y. Lin, P.N. Arendt, S.R. Foltyn, Q.X. Jia, J.L. Mac Manus Dris coll, Structural,morphological and magnetic properties of $La_{1-x}Na_yMnO_3$ nanoparticles produced by the solution combustion method Appl. Phys. Lett.841147.(2004).

[4] F. Ben Jemaa, S.H. Mahmood, M. Ellouze, F. Halouani, Critical behavior in Fe-doped manganites $La_{0.67}Ba_{0.22}Sr_{0.11}Mn_{1-x}Fe_xO_3$ $(0 \leq x \leq 0.2)$ Ceram. Int. 41.8191. (2015).

[5] R.Kajimoto, H. Yoshizawa, H. Kawano, H. Kuwahara, Y. Tokura, K. Ohoyama, M. Ohashi, Hole-concentration-induced transformation of the magnetic and orbital structures in $Nd_{1-x}Sr_xMnO_3$.Phys. Rev. B 60.9506.(1999).

[6] H.Y. Hwang, S. W. Cheong, N. P. Ong and B. Batlogg, Spin Polarized Intergrain Tunneling in $La_{2/3}Sr_{1/3}MnO_3$, Phys. Rev.Lett , 77. 2041–2044.(1996).

[7] C.N. R. Rao, R. Mahesh, A. K. Raychaudhuri and R. Mahendiran, Giant magnetoresistance, charge orderingand other novel properties of perovskite manganates, J. Phys.Chem.Solids,59.487.501.(1998).

[8] B. C. Toeld and W. R. Scott, Oxidative nonstoichiometry in perovskites, an experimental survey; the defect structure of an oxidized lanthanum manganite by powder neutron diffraction, J. Solid State Chem 10. 183–194. (1974).

[9] N. Zhang, W. Ding, T. Tanx, W. Zhong and Y. Du, Simultaneous observation of tunnel-type GMR and intrinsic CMR in nanometer perovskite, Sci. China, Ser. A: Math., Phys.,Astron. 41, 967–973.(1998).

[10] Y. Endoh, K. Hirota, S. Ishihara, S. Okamoto, Y. Murakami A. Nishizawa, T. Fukuda, H. Kimura, H. Nojiri, K. Kaneko and S. Maekawa, Transition between Two Ferromagnetic States Driven by Orbital Ordering in $La_{0.88}Sr_{0.12}MnO_3$ Phys. Rev. Lett, 82, 4328 4331.(1999).

[11] Y. Yamada, O. Hino, S. Nohdo, R. Kanao, T. Inami and S. Katano, Polaron Ordering in Low-Doping $La_{1-x}Sr_xMnO_3$ Phys. Rev. Lett.77. 904–907.(1996).

[12] S. Uhlenbruck, R. Teipen, R. Klingeler, B. Buchner, O. Friedt, M. Hucker, H. Kierspel, T. Niemoller, L. Pinsard A. Revcolevschi and R. Gross, Interplay between Charge Order, Magnetism, and Structure in $La_{0.875}Sr_{0.125}MnO_3$ Phys. Rev. Lett.82.185–188.(1999).

[13] A. Moreo, S. Yunoki and E. Dagotto, Phase separation scenario for manganese oxides and related materials, Science.283.2034–2040.(1999).

[14] Goodenough, J.B. Theory of the Role of Covalence in the Perovskite-Type Manganites [La, M(II)]MnO_3Phys.Rev.100.564.(1955).

[15] Mahendiran, R., Tiwary, S.K., Raychaudhuri, A.K, Ramakrishnan, T.V.Mahesh.R. Rangavittal, N., Rao, C.N.R: ELECTRON SPIN RESONANCE AND RESISTIVITY STUDIES OF CHARGE-ORDERED Bi_{1-x} $Ca_{1-x}MnO_3$ Phys. Rev. B. 53.3348 (1996).

[16] Rodriguez-Martinez, L.M., Attfield, J.P. Cation disorder and the metal-insulator transition temperature in manganese oxide perovskites Phys. Rev. B.58.2426.(1998).

[17] Fan, J., Pi, L., Tong, W., Xu, S., Gao, J., Zha, C., Zhang, Y; Percolative conductivity in the $La_{0.67}Sr_{0.33}Mn_{1-x}Mg_xO_3$ system; Phys.Rev. B. 68.092407. (2003).

[18] Phan, M.H., Morales, M.B., Bingham, N.S., Srikanth, H., Zhang, C.L., Cheong, S.W: Phase coexistence and magnetocaloric effect in $La_{5/8-y}Pr_yCa_{3/8}MnO_3$ (y=0.275) Phys. Rev. B. 81.094413 .(2010).

[19] M. Noumi, Y. Marouani, R. Dhahri, E. Dhahri, E.K. Hlil, B.F.O. Costa Theoretical and experimental studies of the magnetocaloric effect on lacunar compounds, Journal of Alloys and Compounds 157541.(2020).

[20] H. M. Rietveld Line profiles of neutron powder-diffraction peaks for structure refinement Acta Crystallogr 22. 151.(1967).

[21] A. M. Tishin: Ed. Buschow K. H. J, North Holland, Amsterdam, Enhanced magnetocaloric effects and tunable thermal hysteresis in transition metal pnictides HandBook of Magnetic Material Vol.12.(1999).

[22] K. Huang, Statistical Mechanics, 2nd ed, Wiley, New York, (1987).

[23] M. Khlifi, A. Tozri, M. Bejar, E. Dhahri, E.K. Hlil, Effect of calcium deficiency on the critical behavior near the paramagnetic to ferromagnetic phase transition temperature in $La_{0.8}Ca_{0.2}MnO_3$ oxides J. Magn. Magn. Mater, 324. 2142. (2012).

[24] M. Ziese, J. Phys. Critical scaling and percolation in manganite films Condens. Matter. 13.2919. (2001).

[25] M. Nasri ,M. Triki , E. Dhahri , E.K. Hlil, Critical behavior in Sr-doped manganites $La_{0.6}Ca_{0.4-x}Sr_xMnO_3$ .J. Alloys Comp, 546.84.(2013).

[26] Nisha, P, Savitha Pillai, S, Darbandi, A, Varma, M.R, Suresh, K.G., Hahn, H.: Critical behavior and magnetocaloric effect of nano crystalline $La_{0.67}Ca_{0.33}Mn_{1-x}Fe_xO_3$ (x=0.05, 0.2) synthesized by nebulized spray pyrolysis. Mater. Chem. Phys.136.66–74.(2012).

[27] Ben Jemaa, F., Mahmood, S.H., Ellouze, M., Hlil, E.K., Halouani, F.: Critical behavior in Fe-doped manganites $La_{0.67}Ba_{0.22}Sr_{0.11}Mn_{1-x}Fe_xO_3$ ($0 < x < 0.2$). J. Mater. Sci. Mater. Electron. 49.6883–6891.(2014).

[28] Ghosh, K., Lobb, C.J., Greene, R.L.: Critical phenomena in double exchange ferromagnet La0.7Sr0.3MnO3. Phys. Rev. Lett. 81.4740–4743.(1988).

[29] Naoyuki Tateiwa, Jiří Pospíšil, Yoshinori Haga, and Etsuji Yamamoto1, Critical behavior of magnetization in URhAl: Quasi-two-dimensional Ising system with long-range interactions PHYS. REV.B, 97.064423.(2018)**.**

[30] A. Arrott, Criterion for Ferromagnetism from Observations of Magnetic Isotherms Phys. Rev, 108.1394.(1957).

[31] A. Arrott, John E. Noakes, Approximate Equation of State For Nickel Near its Critical Temperature Phy. Rev. Lett, 19 .786. (1967).

[32] J. S. Kouvel, M. E. Fisher, Detailed Magnetic Behavior of Nickel Near its Curie Point Phys. Rev, 136.626. (1964).

[33] S.K. Banerjee, On a generalised approach to first and second order magnetic transitions Phys. Lett. 12.16. (1964).

[34] A. Arrott et John E. Noakes, Approximate Equation of State For Nickel Near its Critical Temperature Phy. Rev. Lett. 19.786.(1967).

[35] H. Oesterreicher, F.T. Paker, Magnetic cooling near Curie temperatures above 300 K J. Appl. Phys.55.4334.(1984).

[36] V. Franco, J.S. Blázquez, The influence of Co addition on the magnetocaloric effect of Nanoperm-type amorphous alloysA. Conde, Appl. Phys. Lett.89.222512.(2006).

[37] Q.Y. Dong, H.W. Zhang, J.R. Sun, B.G. Shen, V. Franco, A phenomenological fitting curve for the magnetocaloric effect of materials with a second-order phase transition J. Appl. Phys.103.1161(2008).

[38] A. Dhahri, E. Dhahri, E.K. Hlil, Structural characterization, magnetic properties and magnetocaloric effects of La0.75Sr0.25Mn1–xCrxO3 (x 5 0.15, 0.20, and 0.25) Appl. Phys. A 116.2077.(2014).

[39] V. FrancoA. Conde, M.D. Kuzmin, J.M. Romero-Enrique, Magnetic field dependence of magnetic entropy change in nanocrystalline and polycrystall inmanganites $La_{1-x}M_xMnO_3$ (M=Ca,Sr)J. Appl. Phys.105. 917.(2009).

[40]. B. Widom, Equation of State in the Neighborhood of the Critical Point J. Chem. Phys. 43.3898.(1965).